Materials Today Chemistry 22 (2021) 100626

Contents lists available at ScienceDirect

Materials Today Chemistry

journal homepage: www.journals.elsevier.com/materials-today-chemistry/

Evaluation of PEGylated fibrin as a three-dimensional biodegradable scaffold for ovarian tissue engineering

A. Dadashzadeh , S. Moghassemi , C.A. Amorim *

Pôle de Recherche en Gynécologie, Institut de Recherche Expérimentale et Clinique, Université Catholique de Louvain, Brussels, Belgium

ARTICLE INFO

Article history:
Received 26 May 2021
Received in revised form
8 September 2021
Accepted 1 October 2021
Available online xxx

Keywords:
PEGylated fibrin
PEGylation
Ovarian tissue engineering
Fibrinogen
Thrombin
Biodegradation

ABSTRACT

The most challenging task of creating a bioengineered ovary to restore fertility in cancer patients is choosing an appropriate biomaterial to encapsulate isolated preantral follicles and ovarian cells. In this study, as a biocompatible and biodegradable biomaterial containing fibrin-like bioactivity and manageable physical properties, PEGylated fibrin aims to encapsulate isolated ovarian stromal cells as a first step of creating an engineered ovarian tissue. For this purpose, human ovarian stromal cells were isolated from frozen-thawed ovarian tissue and cultured in the PEGylated fibrin hydrogels (PEG:Fib), which were fabricated by combining two different molar ratios of PEG:Fib (10:1 and 5:1) and two thrombin concentrations. The samples were analyzed at days 0 and 5 of in vitro for cell density, proliferation (Ki67), and apoptosis (caspase-3). Moreover, LIVE/DEAD and PrestoBlue assays assessed cell viability and proliferation on days 1, 3, and 5. The effect of PEGylation on the biodegradation behavior of fibrin was evaluated by measuring the remaining mass ratio of non-modified fibrin, PEG:Fib 10:1, and PEG:Fib 5:1 hydrogels after 1, 2, 3, 5, 8, 11, and 15 days. The results showed that PEGylated fibrin hydrogels enhanced scaffold stability and supported cell viability and proliferation. In addition, PEG:Fib 5:1 T50 indicated a significantly higher cell density dynamic and non-significantly lower expression of caspase-3 on day 5. Besides, uniformity of cell distribution inside the hydrogel and a tendency to a high rate of Ki67-positive cells was observed in PEG:Fib 10:1 T50 hydrogels. In conclusion, this study reveals the positive effects of PEGylated fibrin hydrogels on isolated human ovarian stromal cells. Based on such promising findings, we believe that this matrix should be tested to encapsulate isolated human ovarian follicles.

1. Introduction

Tissue engineering is a promising approach to repair, replace, or improve the damaged or whole organ or tissue [1,2]. Based on its principles, we aim to assemble an engineered artificial ovary to preserve fertility in young female cancer patients who cannot undergo any of the current alternatives due to the possible presence of malignant cells in their cryopreserved ovarian fragments [3]. To this end, we must develop a three-dimensional (3D) biocompatible and biodegradable scaffold to support follicle survival and growth by preserving its 3D structure, the proliferation of granulosa, theca, and stromal cells, as well as oocyte maturation [4–7]. Although fibrin hydrogel was vastly used for fabricating a tissue-engineered ovary [3,8–14], there is a primary limitation associated with rapid degradation of fibrin, which leads to loss of implant volume within days and subsequently losing physical support for the cells encapsulated in the hydrogels [15–18]. In order to overcome this limitation, some approaches can be applied, such as combining fibrin with other biomaterials, using enzymes or chemical modifications, such as PEGylation, to control the fast hydrogel biodegradation [19–22].

PEGylation is a chemical enhancement process in which polyethylene glycol (PEG) attaches to a target protein structure to enhance fibrin biodegradability and stability [16,23,24]. PEG molecules with their large hydrodynamic radius act as shields in front of proteases and reduce proteolysis of proteins [25,26]. For instance, an active and biocompatible PEG can improve fibrin mechanical strength by reacting with the amino groups of fibrinogen [27,28], as demonstrated by the higher storage modulus of PEGylated fibrin compared to non-modified fibrin [29]. Indeed, PEGylation can modify fiber morphology, which affects hydrogel stiffness [29]. Furthermore, Seetharaman et al. [30] indicated that

* Corresponding author.
E-mail address: christiani.amorim@uclouvain.be (C.A. Amorim).

https://doi.org/10.1016/j.mtchem.2021.100626
2468-5194/

PEGylated fibrin mixed with microspheres formed stable structures without decreasing the storage modulus up to 72 h.

Another advantage of PEGylation is that it renders fibrin gels clear in the visible light, allowing the study of cell behavior encapsulated in the hydrogel [31]. This transparency property could be due to the size of PEGylated fibrin conjugates, which are smaller aggregates than fibrin and the turbidity analysis showed that the PEGylated fibrin could transmit 66% and 98% of visible light at the wavelengths of 380 and 780 nm, respectively [31].

Despite PEGylated fibrin advantages [16,24,30,32–35] and its wide application in tissue engineering [34,36–41], there is no report of using this hydrogel in ovarian tissue engineering. Therefore, the goal of this study is to provide an initial analysis of PEGylated fibrin hydrogels based on their degradation and ability to support the survival and proliferation of human ovarian cells in vitro. To this end, we chose two different molar ratios of PEG and fibrinogen (10:1 and 5:1), which were synthesized and clotted with two different concentrations of thrombin (Fig. 1). These two molar ratios were chosen based on previous studies showing that molar ratios higher than 10:1 led to a significant decrease in amine groups and an increase in gelation time [22]. Moreover, the effect of thrombin content as an active component was evaluated on the final clotted gels characterization.

2. Materials and methods

2.1. Synthesis of PEGylated fibrinogen

Human fibrinogen (F3879; Sigma-Aldrich, Bornem, Belgium) was solubilized in Dulbecco's phosphate buffered saline (DPBS; 14040-091; Gibco, Merelbeke, Belgium) at a concentration of 85 mg/mL. After 2 h incubation at 37°C, the solution was filtered using a 0.20-mm syringe filter (16534-K; Sartorius, Goettingen, Germany). O,O'-Bis[2-(N-Succinimidyl-succinylamino)ethyl]polyethylene glycol (NHS-PEG-NHS; 2,000 Da; 713783; Sigma-Aldrich) solution in DPBS was prepared at 5 mg/mL and syringe filtered. NHS-PEG-NHS solution was added to the fibrinogen in 1:1 and 1:2 vol ratios to create 10:1 and 5:1 M ratios of PEGylated fibrinogen (PEG:Fib 10:1 and PEG:Fib 5:1), mixed thoroughly, and incubated at 37°C. A proper volume of DPBS was added to the PEG:Fib 5:1 after 1 h incubation to have the final concentration of 45 mg/mL. In addition, non-modified fibrinogen with a concentration of 45 mg/mL was prepared.

2.2. Degradation analysis of hydrogels

Human thrombin (T7009; Sigma-Aldrich) was reconstituted and diluted in 40 mM $CaCl_2$ (C5080; Sigma-Aldrich) to achieve concentrations of 25 and 50 IU/mL (T25 and T50) and incubated at 37°C before use. Equal volumes of T25 and T50 were added to non-modified fibrinogen, PEG:Fib 10:1, and 5:1 droplets into the glass bottles and incubated at 37°C for 15 min to produce fibrin and PEG:Fib hydrogels. After incubation, the initial weight (W_i) of samples was weighed. Then, DPBS was added to the tubes containing hydrogels, and the medium was changed every second day. After 1, 2, 3, 5, 8, 11, and 15 days, DPBS was removed from the bottles and the hydrogels were allowed to dry for a few minutes before weighing. The remaining mass (W_r) could be assessed after subtracting the glass bottle's weight, which was measured before hydrogel synthesis. The hydrogel degradation was investigated gravimetrically, and the remaining mass ratios were achieved by the following formula: $(W_r/W_i) \times 100$ [42,43].

The enzymatic degradation of PEGylated fibrin hydrogels was analyzed colorimetrically based on Dikovsky et al. [37] protocol. Briefly, PEGylated fibrin hydrogels were stained using 5 mg/mL eosin-Y (1.15935.0025; Merck) for 2 days and after consecutive washing with DPBS, 2 mL of enzymatic digestion solution containing 50 mM phosphate buffered saline (PBS; 524650-1EA; Merck, Sigma-Aldrich), 0.1 mg/mL collagenase (C2674; Sigma-Aldrich), and 0.1% sodium azide was added to each hydrogel.

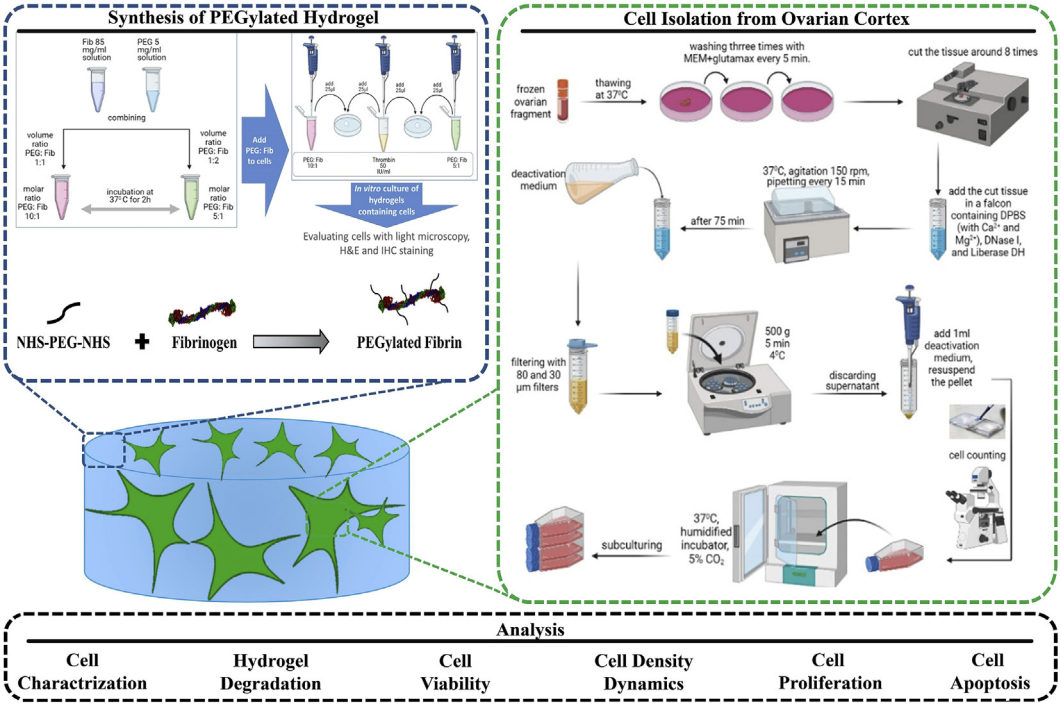

Fig. 1. Workflow of experiments.

Every 30 min, the protein release in the solution was quantified spectrophotometrically at 490 nm for 3 h. At each time point, 100 μL of hydrogel medium was removed for spectrophotometrical analysis, and the same volume of a new enzymatic solution was added. The absorbance of fully degraded hydrogel media was considered as 100% to normalize the results.

2.3. Isolation and in vitro culture of ovarian stromal cells

The ovarian tissue biopsies were obtained after approval from the Institutional Review Board of the Université Catholique de Louvain for the use of human ovarian cortex in May 2019 (IRB reference 2012/23MAR/125, registration number B403201213872). The dissected ovary was directly transported to the laboratory in minimum essential medium (42360-024; Gibco) at 4°C. After removing the medullar part, the cortex was frozen using our routine procedure [44]. The ovarian stromal cells were isolated after thawing [44] of the ovarian tissue fragments, according to Asiabi et al. [45]. Briefly, the tissue was minced with the use of a McIlwain tissue chopper (Campden Instruments, Loughborough, UK) adjusted to 0.5 mm and then digested with Liberase DH (5401054001; Sigma-Aldrich) and DNAse I (10104159001; Sigma-Aldrich) at 37°C for 75 min. Then, the enzymatic digestion was inactivated by adding an equal amount of DPBS supplemented with 10% heat-inactivated fetal bovine serum (FBS; 16140-071; Gibco). Afterward, the suspension was filtered through 80 (NY8002500; Millipore, Sigma-Aldrich) and 30 μm (NY3002500; Millipore) nylon net filters and centrifuged (500 *g*, 10 min). The pellet was resuspended in culture medium, which consisted of Dulbecco's modified Eagle medium F-12 nutrient mixture (21041-025; Gibco) supplemented with 10% heat-inactivated FBS and 1% of antibiotic and antimycotic (Anti-Anti; A5955; Gibco), and after cell counting with trypan blue (T8154; Sigma-Aldrich) and a Bürker chamber, the cells were in vitro cultured at 37°C in a humidified incubator with 5% CO_2. The culture medium was changed every other day, and cells were subcultured after reaching confluence.

2.4. Polychromatic flow cytometry

In order to identify the cell populations, the isolated cells were prepared for flow cytometry following Feisst et al. [46] protocol. Frozen-thawed cells were washed and incubated in the culture medium at 37°C, 5% CO_2 for 1 h before staining. Then, they were washed with PBS and stained with the following antibodies: CD90 (328113; BioLegend, Amsterdam, The Netherlands), CD73 (344007; BioLegend), CD326 (324233; BioLegend), CD 34 (343615; BioLegend), and CD31 (303131; BioLegend) and incubated at room temperature for 10 min. Samples were run on the BD FACSCanto™ II Clinical Flow Cytometry System (BD Biosciences, Erembodegem, Belgium), and data were analyzed using FlowJo software (BD Biosciences, Ashland, USA).

2.5. Preparation of hydrogel-encapsulated ovarian stromal cells

Passage 1–2 cells were used for embedding in hydrogels. After detaching cells with 0.05% trypsin-ethylenediaminetetraacetic acid (EDTA) (1×) (25300, Gibco) and counting them, the appropriate number of cells was added in three tubes, centrifuged, and after discarding the supernatant, they were resuspended in PEG:Fib 10:1, PEG:Fib 5:1, and fibrinogen to have a cell density of 8×10^5 cells/mL. A droplet of different hydrogels containing stromal cells was deposited on a four-well plate (179830; Thermo Scientific, Merelbeke, Belgium). The equal amount of thrombin (at 25 or 50 IU/mL) was mixed with the droplet and incubated at 37°C for 15 min. After polymerization, 1 mL culture medium was added to each well, and it was changed every second day. Stromal cells embedded in the hydrogels were cultured for 5 days at 37°C in a humidified incubator with 5% CO_2.

2.6. Viability analysis

Cell viability evaluation on days 1, 3, and 5 was performed by using LIVE/DEAD™ viability/cytotoxicity kit (L3224; Invitrogen, Merelbeke, Belgium), containing calcein-AM dye and ethidium homodimer-1 to indicate live (green) and dead (red) cells, respectively. After removing cell culture medium and rinsing hydrogels with DPBS, the constructs were incubated in 500 μL of dye solution, composed of 0.5 μL of calcein-AM and 2.5 μL of ethidium homodimer-1 in 997 μL DPBS, for 45 min at 37°C. Then, the hydrogels were transferred to a microscopic slide and covered with a coverslip to visualize the cells using a fluorescent microscope (Leica DMIL, Diegem, Belgium). Green fluorescence was visualized in live cells (ex/em 495/515 nm) and red fluorescence in dead cells (ex/em 495/ 635 nm), using two different filters.

Cell mitochondrial activity on days 0, 1, 3, and 5 was analyzed by PrestoBlue™ HS cell viability reagent (P50200; Invitrogen) according to the manufacturer protocol. Briefly, after aspirating the medium, PrestoBlue (diluted 1:10 in the cell culture medium) was added to wells containing cell-encapsulated and cell-free hydrogels and left to incubate for 3 h at 37°C. A total of 100 μL of the medium in each well was transferred to a 96-well plate, and fluorescence was measured by fluorescence spectroscopy (Multilabel reader; Victor X4, Singapore) with the emission wavelength at 620 nm and the excitation wavelength at 560 nm. The average fluorescence value of the medium in the cell-free hydrogel as a background was subtracted from the values obtained from the same hydrogel-contained cells. Data were analyzed by SPSS® software (IBM, Chicago, USA), and the increasing rate of fluorescence values was obtained by dividing the fluorescence values of samples on different days to day 0.

2.7. Histological and immunohistochemical analyses

Soon after hydrogel polymerization (day 0 samples) and after 5 days of in vitro culture (day 5 samples), each combination of hydrogels was embedded in HistoGel (HG-4000-012; Thermo Scientific), immediately fixed in 4% paraformaldehyde (VWR, Leuven, Belgium) at room temperature for at least 3 h and then transferred into 70% ethanol at 4°C for at least 24 h. After dehydration and clarification, the hydrogels were embedded in paraffin, cut into the serial sections of 7 μm, and every fourth section was stained with hematoxylin and eosin (Hx61057849 and Hx87833544; Merck) for morphological analysis, while the remaining sections (Superfrost®Plus; Menzel-Glaser, VWR) were kept for immunohistochemistry.

To locate stromal cells and calculate cell density at days 0 and 5, three different sections of each sample were examined at 200× magnification, digitized by a Leica DFC295 camera and imaging program (Leica Application Suite; Leica). Total cells in a $200 \times 200\ \mu m^2$ area were counted and measured by ImageJ (https://imagej.nih.gov/ij/). The dynamic percentage of cell density (C_d) after 5 days of in vitro culture was determined by the following equation [13]:

$$C_d = \frac{\text{density of day 5} - \text{density of day 0}}{\text{density of day 5}} \times 100$$

Immunohistochemical analysis was performed for caspase-3 and Ki67 antibodies on consecutive tissue sections to assess apoptosis and proliferation activity of the encapsulated stromal cells in the hydrogels. Briefly, tissue sections were deparaffinized and rehydrated, followed by endogenous peroxidase inhibition

using hydrogen peroxide 30 min at room temperature. Antigen retrieval was done in a water bath at 98°C for 75 min, and non-specific protein inhibition was performed using 1% bovine serum albumin, and 10% FBS solution in Tris-buffered saline for 30 min at room temperature. Subsequently, the sections were incubated in a humidified chamber at 4°C overnight with either polyclonal (rabbit) anti-caspase-3 (9661S; 1:200; Cell Signaling, Leiden, The Netherlands) or monoclonal anti-human Ki67 (M7240; 1:100; DAKO, Glostrup, Denmark). After washing three times with a washing solution containing Tris-buffered saline and 20% Triton X-100, the sections were incubated for 1 h at room temperature in either Envision anti-rabbit System HRP (K4003; DAKO) or Envision anti-mouse System HRP (K4001; DAKO). After rinsing with washing solution, slides were incubated with the 3,3'-diaminobenzidine chromogen (Vector, Labconsult, Brussels, Belgium) for 15 min at room temperature and subsequently counterstained with hematoxylin for 30 s, followed by dehydration in isopropanol and mounting for further analyses. Human tonsil and endometrium were used as positive controls for caspase-3 and Ki67 analysis, respectively. The positive cells in each staining were counted in a 200 × 200 μm^2 area, and the percentage of caspase-3- and Ki67-positive cells on day 5 was calculated.

2.8. Statistical analysis

Statistical analyses on the data of the degradation test, in vitro cell culture experiments, and histological/immunohistochemical analyses were performed using a one-way analysis of variance combined with post hoc Tukey–Kramer Multiple Comparisons test. Calculations were performed in JMP® Pro 15.2.0 (SAS Institute Inc., NC) software. The statistical data were presented as mean ± standard deviation, and the level of significance was taken at a p-value of 0.05.

3. Results and discussion

3.1. Degradation evaluation of the fibrin hydrogels

The degradation/dissolution behavior of the different types of hydrogels is illustrated in Fig. 2. Our findings showed that in contrast to PEGylated fibrin matrices, fibrin formulations with both thrombin concentrations dramatically lost their total weights after 5 days. The PEGylated fibrin hydrogels compared to non-modified fibrin hydrogels indicated significantly higher stability with a gradual degradation rate, preserving around 70–80% of their mass after 15 days of incubation in DPBS solution at 37°C. The degradation rate for PEG:Fib 10:1 T50 and PEG:Fib 5:1 T25 was similar, with a gradual decline in their remaining mass ratio. The remaining mass of PEG:Fib 10:1 T25 was significantly superior to PEG:Fib 5:1 T50 and PEG:Fib 5:1 T25 ($p<0.05$) on day 5. However, comparing different PEGylated fibrin hydrogels showed no significant differences on the other days.

Although the non-modified fibrin hydrogels were subjected to intense degradation, the chemically modified counterparts enhanced the matrix stability behavior and slowed down their mass loss (Fig. 2a). Indeed, PEGylation improves the stability of proteins by increasing their molecular size and weight [31,47,48] and decreasing the accessibility of biomolecules to them [49]. Moreover, PEGylation reduces the charge of proteins by either changing amine groups to amide or masking the surface charges [50]. Therefore, PEGylation may decrease ionic interactions between fibrin and DPBS and shields fibrin from rapid dissolution and degradation.

Interestingly, we observed a tendency for a positive correlation between thrombin concentration and matrix degradation ratio. This result is consistent with studies indicating that the increasing thrombin concentrations in fibrin hydrogels decrease matrix fiber thickness, leading to faster degradation [51–53]. Indeed, higher thrombin concentrations reduce gelation time and produce thinner fibers [54]. Because thin fibers are cleaved quicker than their thick counterparts, fibrin hydrogels made of them are dissolved at a faster rate [54]. However, it is important to bear in mind that fibrin degradation is a complex phenomenon related not only to fiber diameter but also to other conditions, such as fiber density (amount of protein per volume), pore size, and accessibility of inner fibers [55].

As Fig. 2b reveals, the PEGylation could enhance not only fibrin stability but also its transparency. Indeed, while PEGylated fibrin matrices were found until the last day of incubation, non-modified fibrin hydrogels were completely degraded in less than 1 week (Fig. 2b). Moreover, the translucence of PEGylated fibrin hydrogels allowed precise observation of the cells under the inverted microscope, which was not possible with non-PEGylated matrices.

Fig. 2c indicates the enzymatic degradation of PEGylated fibrin in 0.1 mg/mL collagenase. Collagenase was chosen for the enzymatic degradation of hydrogels to have a general evaluation of PEGylated fibrin degradability, as this enzyme has been widely applied for this purpose [56–58]. Different PEGylated fibrin hydrogels demonstrated approximately similar degradation rates within 3 h, which they release around 40–60% bulk protein to medium in the last time point. This degradation was obtained from proteolysis and strength ionic reactions, in which collagenase and 50 mM PBS were responsible for enzymatic and ionic degradation, respectively. However, the swelling ratio of the hydrogels could be an error in this experiment. Because the successive washing could not completely remove eosin from porosities, the colorimetric analysis could result from both releasing eosin-labeled proteins and entrapped eosin molecules in the porosities. It seems that PEGylated fibrin hydrogels (PEG:Fib 10:1 T25, 5:1 T50) that indicated a more swelling ratio at day 1 (Fig. 2a) represented more enzymatic degradation, as well (Fig. 2c). However, there is no significant difference between the results.

3.2. Characterization of the cell populations

A panel of five markers was used for polychromatic flow cytometry, including CD326, CD31, CD34, CD70, and CD90. Only 0.73 ± 0.35% of cells were CD326+. After excluding CD326+ cells, the CD326−, CD31−, and CD34+ (Q1); CD326−, CD31+, and CD34+ (Q2); CD326−, CD31+, and CD34− (Q3); and CD326−, CD31−, and CD34− (Q4) were 26.75 ± 7.96%, 12.87 ± 6.8%, 2.84 ± 2.6%, and 57.55 ± 4.06%, respectively (Fig. 3). The Q3 and Q4 showed the minimum and maximum values of cell populations (Q4 vs. Q3, Q2, and Q1 $p<0.0001$; Q3 vs. Q1 $p<0.0001$). Each gate had more than 5% analyzed for CD73 and CD90 (Table 1).

As results demonstrate, the percentage of epithelial cells (CD326+) is neglectable. Moreover, isolated ovarian stromal cells from the cortex indicated a probability of less endothelial type cells (Q3: 2.84%), 26.75% progenitor cells, or maybe hematopoietic stem cells (Q1) and some endothelial progenitor cells (Q2: 12.87%) but 57.55% of mesenchymal or fibroblast cells (Q4). Around 50% and 38% of Q1 and Q2, respectively, were CD90−, indicating that this percentage of Q1 was not hematopoietic stem cells, as these cells express CD90 and CD34 [59]. Considering that the minimal essential markers to classify mesenchymal cells are CD34−, CD73+, CD90+, and CD105+ [60], our results indicate that 16.31% of cells in Q4 may be mesenchymal or fibroblast cells, which are CD34−, CD73+, and CD90+. However, it would be necessary to add CD105 staining to discuss these cells' phenotypes better. Furthermore, the Q1 and Q2 indicated 45.82% and 52.15% of their cells CD90+ and

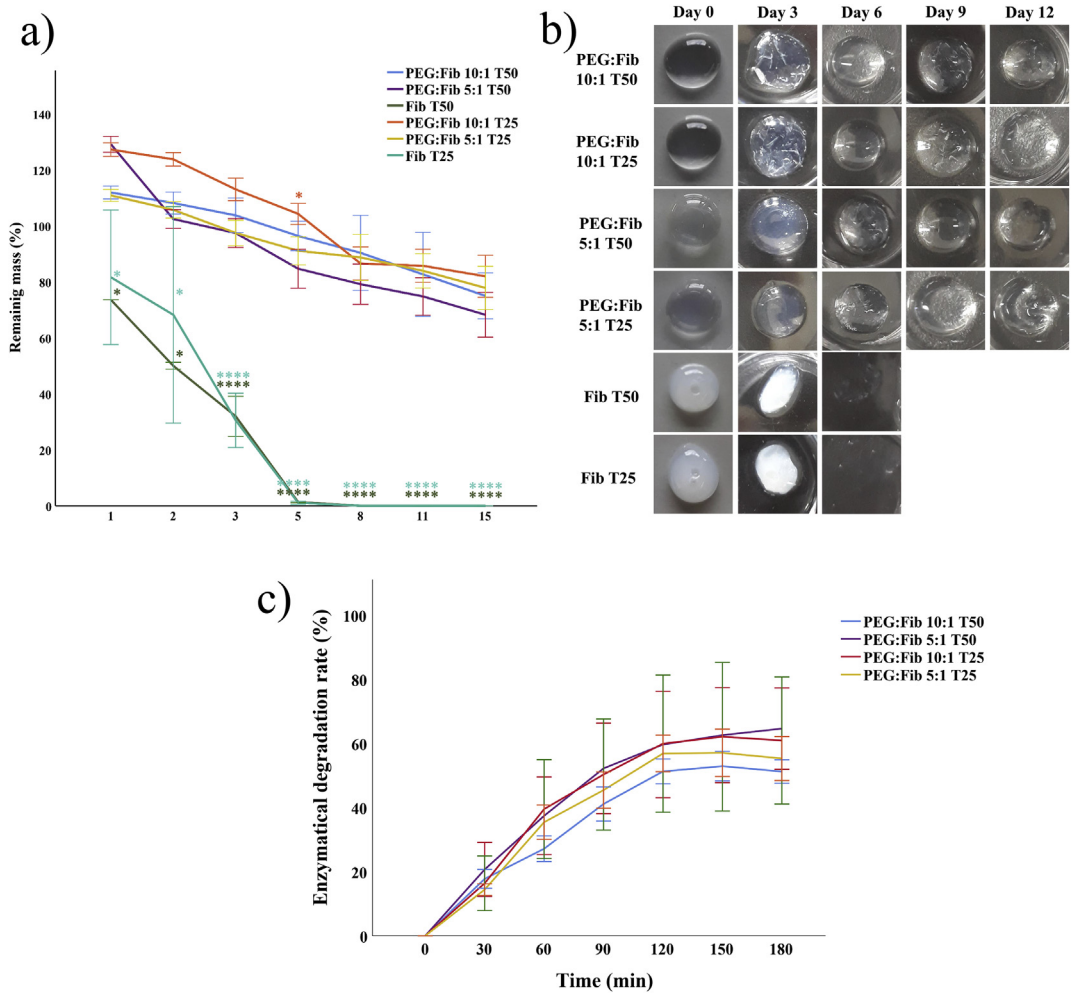

Fig. 2. Degradation and aspect of the fibrin hydrogels. (a) Degradation profiles of PEG:Fib 10:1 T50, PEG:Fib 5:1 T50, PEG:Fib 10:1 T25, PEG:Fib 5:1 T25, Fib T50, and Fib T25 hydrogels, mean ± SD (n = 2). Light and dark green asterisks mark significant differences for non-modified fibrin hydrogels vs. PEGylated fibrin hydrogels; orange asterisks mark the significant difference for PEG:Fib 10:1 T25 vs. PEG:Fib 5:1 T25 and PEG:Fib 5:1 T50 (*p<0.05; ****p<0.0001); (b) appearance and stability of PEGylated and non-modified fibrins on days 0, 3, 6, 9, and 12. After the sixth day of in vitro culture, non-PEGylated fibrin hydrogels had completely dissolved. (c) Enzymatic degradation of PEG:Fib hydrogels, mean ± SD (n = 3).

CD73+. Considering that the Q1 and Q2 gates are CD34+, and the CD73 and CD90 are common antibodies between mesenchymal cells and fibroblasts, the CD73+ and CD90+ cells of Q1 and Q2 may be fibroblast cells. Nevertheless, to confirm that these cells are indeed fibroblasts, podoplanin and CD105 staining would be necessary.

3.3. Cell viability

Cells encapsulated in PEGylated fibrin samples preserved their viability throughout the in vitro culture period (Fig. 4a). On the other hand, in non-modified fibrin samples, due to the significant degradation of the hydrogels, cells were released in the well after 3 days of in vitro culture, and only a few ones remained in the bulk of the matrices. Moreover, the number of viable cells in all PEGylated fibrin groups increased during in vitro culture, especially PEG:Fib 5:1 and 10:1 clotted by T50 hydrogels, which indicated a larger number of viable cells. This result demonstrates the positive effect of the hydrogels on cell proliferation, inducing a rise in the proportion of viable cells, which was also evidenced by PrestoBlue analysis. Indeed, this assay shows that PEGylated fibrin scaffolds induced cell proliferation and activity over time. The mitochondrial activity of encapsulated cells was higher in the PEG:Fib 5:1 T50 hydrogels on day 5 (vs. PEG:Fib 5:1 T25, p<0.0001; vs. PEG:Fib 10:1 T25, p<0.0001; vs. PEG:Fib 10:1 T50, p<0.05) and lower in the PEG:Fib 5:1 T25 hydrogels (vs. PEG:Fib 10:1 T25, p<0.01; vs. PEG:Fib 10:1 T50, p<0.0001). PEG:Fib 10:1 T50 also showed higher fluorescence values compared to PEG:Fib 10:1 T25 (p<0.001) and PEG:Fib 5:1 T25 (Fig. 4b). The viability analyses indicate the ability of PEGylated fibrin to serve as a proper substrate for cell survival and proliferation with different profiles related to the molar ratios of PEG:Fib and thrombin concentrations. Providing a suitable microenvironment for the proliferation of human adipose stromal cells within PEGylated fibrin has been reported in several works of Zhang et al. [22,29,61]. Our results also showed a positive correlation between thrombin concentration and cell proliferation, which has been previously reported in the literature [62–65].

Furthermore, light microscopy analysis of cells encapsulated in PEGylated fibrin hydrogels clotted by T50 indicated more elongated cells in the PEG:Fib 5:1 hydrogel than the PEG:Fib 10:1, which had more rounded shape cells (Fig. 5). The difference in cell morphology between the PEGylated fibrin hydrogels indicates that increasing the molar ratios of PEG:Fib could decrease the bioactivity of fibrin [66]. Indeed, the increasing PEGylation molar ratio decreases the amine groups of fibrin [22], which play a role in cell attachment

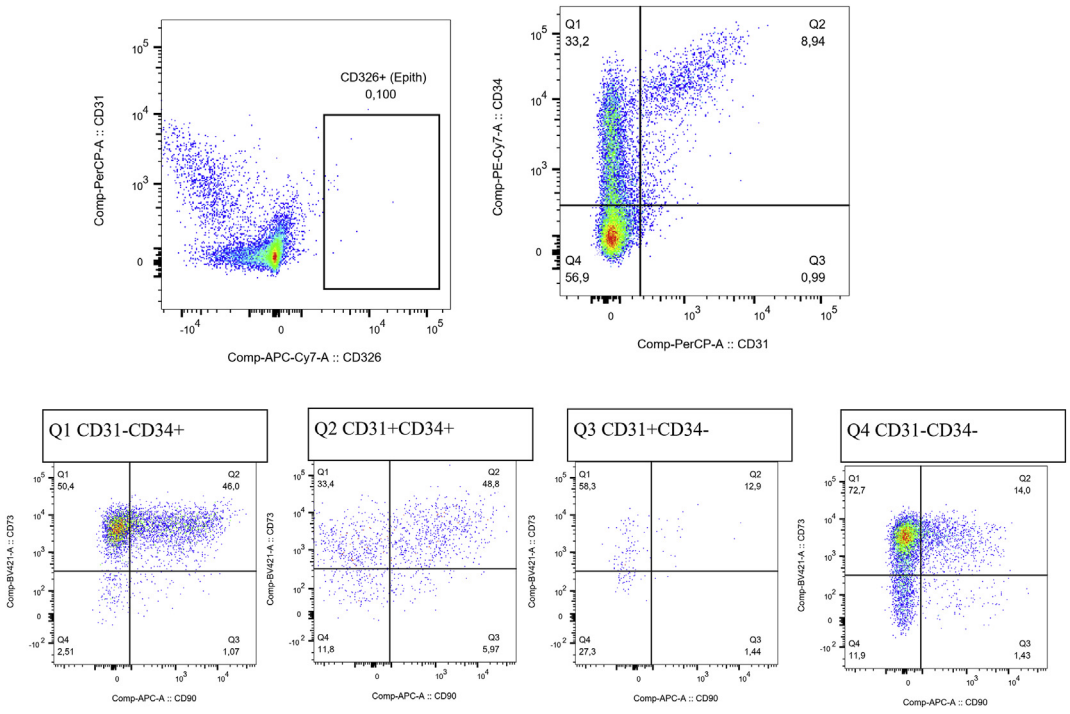

Fig. 3. Flow cytometry analysis of human ovarian cell populations. The panel included CD326, CD31, CD34, CD73, and CD90.

Table 1
Assessing CD90 and CD73 markers in the main gates of Q1, Q2, and Q4.

D90 and CD73	Q1 (average ± SD)	Q2 (average ± SD)	Q4 (average ± SD)
CD90− and CD73+	45.33 ± 16.2	21.37 ± 7.75	50.27 ± 12.82
CD90+ and CD73+	45.82 ± 13.72	52.15 ± 19	16.31 ± 6.02
CD90+ and CD73−	3.65 ± 2.78	9.48 ± 4.76	4.13 ± 1.5
CD90− and CD73−	5.20 ± 5.53	16.98 ± 15.08	29.28 ± 11.97

Q1, CD326−, D31−, and CD34+; Q2, CD326−, CD31+, and CD34+; Q4, CD326−, CD31−, and CD34−; SD, standard deviation.

[67]. Cell morphology could also have been influenced by the denser structure of PEG:Fib 10:1 compared to PEG:Fib 5:1 [34] as compact hydrogels have been shown to induce cell spherical morphology [68].

3.4. Cell density, proliferation, and apoptosis

To investigate cell distribution inside the hydrogels and dynamics of cell density, the PEGylated fibrin hydrogels containing stromal cells were cultured for 5 days, and the samples were fixed after the encapsulation and after in vitro culture as day 0 and day 5 samples, respectively. PEG:Fib 10:1 hydrogels showed more uniformity of cell distribution compared to the PEG:Fib 5:1 hydrogels (Fig. 6). However, the PEG:Fib 5:1 T50 represented significantly higher C_d compared to other hydrogels (vs. PEG:Fib 10:1 T25, $p<0.0001$; vs. PEG:Fib 10:1 T50, $p<0.01$; vs. PEG:Fib 5:1 T25, $p<0.01$) (Table 2). The high cell density dynamics of PEGylated hydrogels indicated their positive effect to support and induce an increase in cell population over time. In addition, PEG:Fib 5:1 T50 exhibited a significantly higher cell density than PEG:Fib 10:1 T25 on day 5 ($p<0.05$) (Table 2). Moreover, cells in the PEG:Fib 5:1 hydrogels were found at the boundary sites, while it appears that with the increasing molar ratio to 10:1, the hydrogels could provide a better distribution of the cells, with more homogenous constructions (Fig. 6).

To determine the effect of the PEGylated fibrin scaffolds on the proliferation and apoptosis status of the ovarian stromal cells, the expression of Ki67 and caspase-3 on day 5 was investigated using immunohistochemical staining (Fig. 6). Again, Ki67 staining confirmed the positive effect of PEGylated fibrin hydrogels on cell proliferation. Additionally, PEG:Fib 5:1 T25 indicated more caspase-3 positive cells than other hydrogels.

As Table 2 demonstrates, despite the lack of significant differences of caspase-3 expression between the 10:1 PEGylated fibrin hydrogels clotted by T25 or T50, the PEG:Fib 5:1 T25 had the highest caspase-3 expression (vs. PEG:Fib 10:1 T50, $p<0.05$; vs. PEG:Fib 10:1 T25, $p<0.01$; vs. PEG:Fib 5:1 T50, $p<0.01$). In addition, there was no significant difference between the results of Ki67 expressions of cells in different hydrogels. Comparing our Ki67 expression and Luyckx et al. [13] results, who encapsulated stromal cells in non-modified fibrin hydrogels, shows that PEGylation can enhance the proliferation index of fibrin matrices.

Comparing the effect of thrombin concentration on the PEGylated fibrin hydrogels reveals a significantly superior cell density dynamics and less caspase-3 expression in PEG:Fib 5:1 T50 against PEG:Fib 5:1 T25 (Table 2). Rowe et al. [54] and Luyckx et al. [13] showed that the thrombin concentration could affect the decreasing rate of sequential cleavage of fibrinopeptides. Indeed, the diameter of fibrin fibers, their compaction, and mechanical properties, measured by scanning electron microscopy,

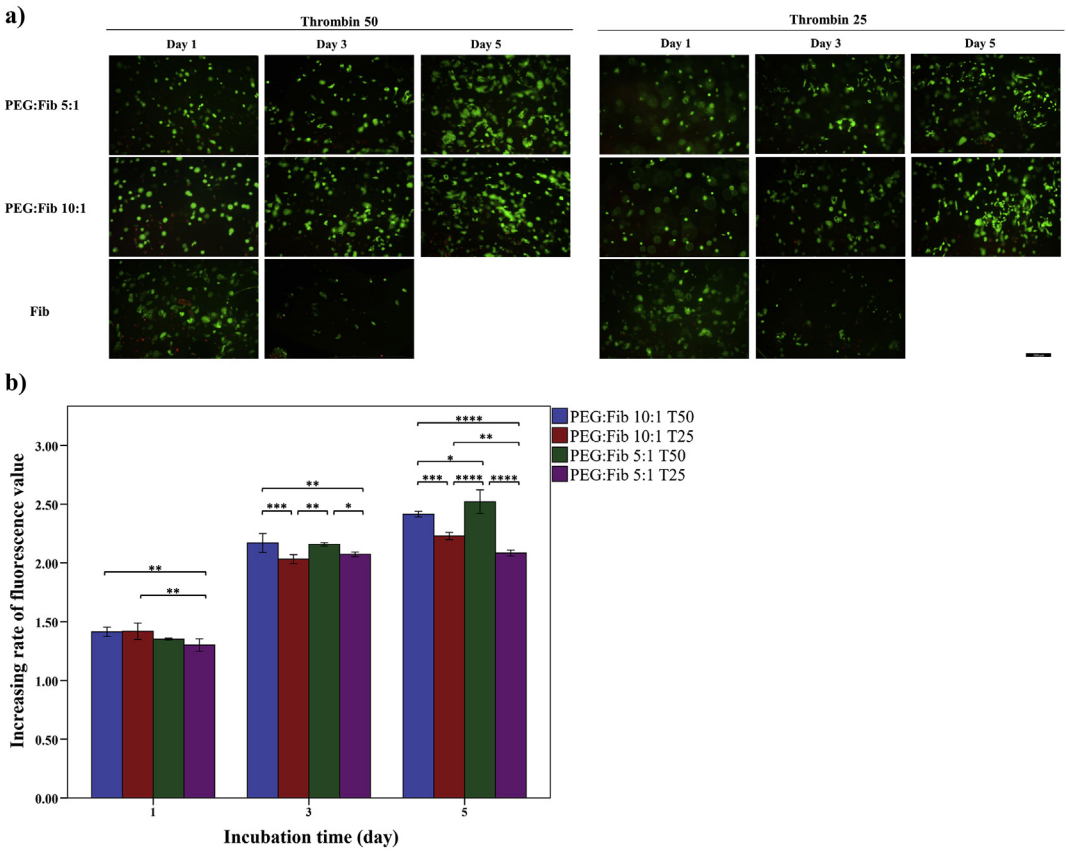

Fig. 4. Cell viability after *in vitro* culture. (a) Fluorescence microscopic images of LIVE/DEAD staining in ovarian stromal cells encapsulated in different hydrogels after 1, 3, and 5 days of in vitro culture. Scale bars indicate 200 μm; (b) graph showing increasing rates of fluorescence values of encapsulated stromal cells in PEGylated fibrin hydrogels at days 1, 3, and 5 by using the PrestoBlue reagent (mean ± SD; n = 3) (*p<0.05; **p<0.01; ***p<0.001; ****p<0.0001). SD, standard deviation.

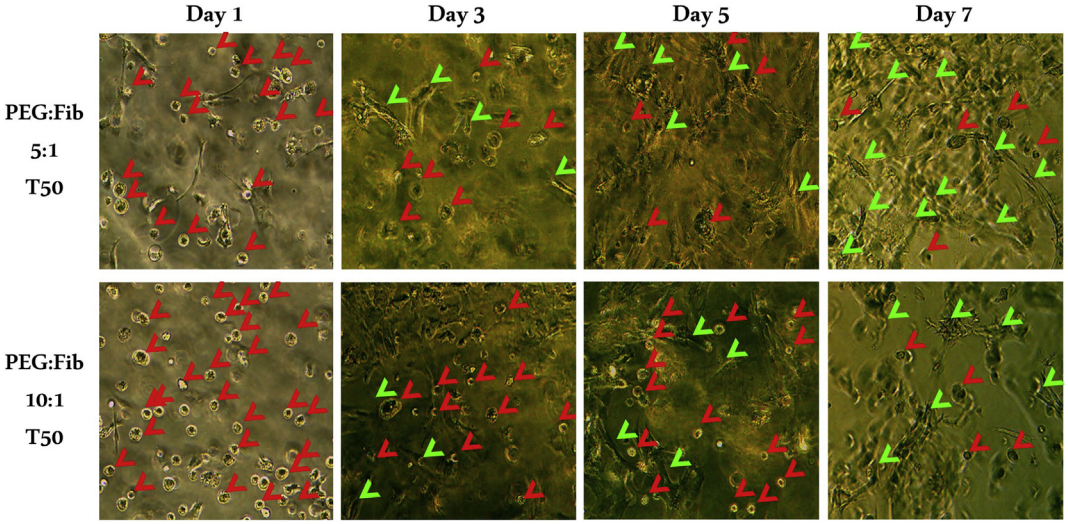

Fig. 5. Light microscopy images of ovarian stromal cells encapsulated in PEGylated fibrin hydrogels clotted by T50. The black and green arrows show round and elongated cells, respectively. Scale bar indicates 200 μm.

digital image analysis, and uniaxial tensile testing system, respectively, increased when the thrombin concentration decreased [54]. Furthermore, when cells are cultured on the fibrin surfaces, they have more projections, i.e., extensions, increasing thrombin concentration [54]. It appears that when fibrin fibers are thinner, the cells can have more connections with fibrin bioactive sites.

On the other hand, the cell proliferation rate obtained by PrestoBlue, as well as cell density of PEG:Fib 5:1 T50 on day 5, were significantly higher than PEG:Fib 10:1 T50. Indeed, although the

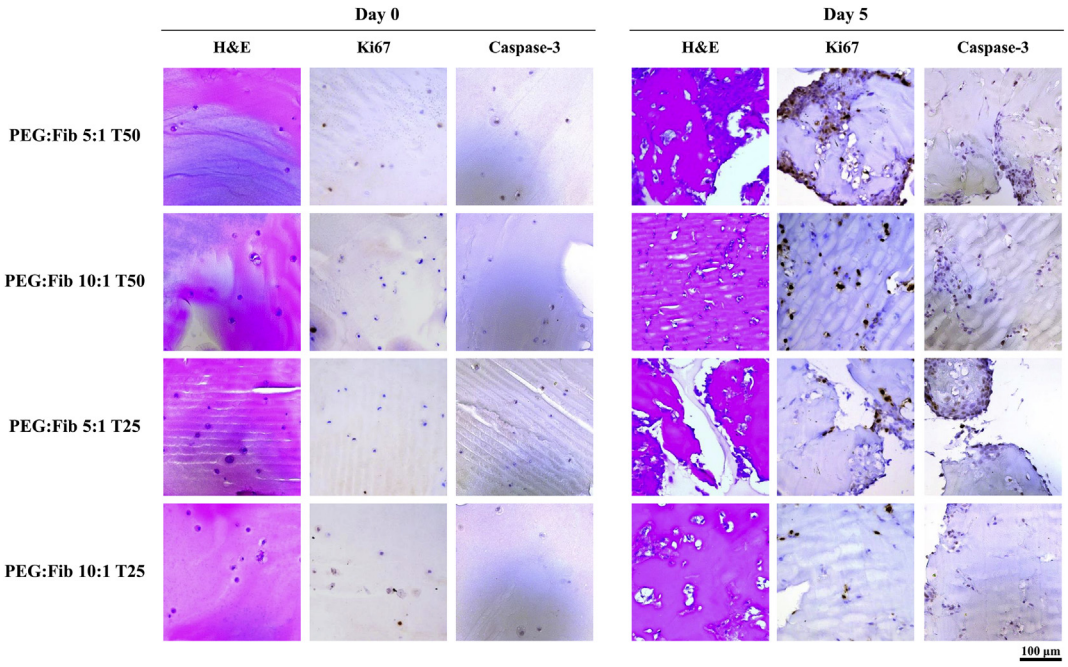

Fig. 6. Histological and immunohistochemical analyses of isolated ovarian stromal cells on day 0 and after 5 days of *in vitro* culture. Positive Ki67 and caspase-3 cells stained brown. Scale bar indicates 100 µm.

Table 2
Analyses of cell density dynamics, caspase-3- and Ki67-positive cells after 5 days of in vitro culture (mean ± SD; n = 4).

Combination	Cell density (%) × 10^{-4}		Cell density dynamics (%)	Caspase-3 expression (%)	Positive caspase cells/area (µm^2) × 10^{-4}	Ki67 expression (%)	Positive Ki67 cells/area (µm^2) × 10^{-4}
	Day 0	Day 5					
PEG:Fib 10:1 T50	2.375 ± 0.661	14.375 ± 4.423^{a,b}	83.341 ± 1.011^{b}	32.389 ± 7.409^{b}	3.062 ± 1.068^{b}	24.018 ± 5.292	6.004 ± 1.323
PEG:Fib 10:1 T25	1.687 ± 0.239	8.937 ± 2.585^{b}	80.276 ± 4.329^{b}	31.722 ± 2.961^{b}	2.125 ± 0.661^{b}	16.479 ± 4.047	4.119 ± 1.012
PEG:Fib 5:1 T50	1.500 ± 0.204	19.562 ± 3.009^{a}	92.303 ± 0.597^{a}	28.137 ± 5.335^{b}	4.375 ± 0.829^{b}	21.572 ± 5.335	5.393 ± 1.333
PEG:Fib 5:1 T25	2.000 ± 0.612	13.937 ± 6.684^{a,b}	84.771 ± 2.469^{b}	47.838 ± 6.182^{a}	8.062 ± 2.303^{a}	23.134 ± 8.820	5.783 ± 2.205

Different letters in the same column indicate the statistical difference between groups (p<0.05).

PEGylation preserves the fibrin against fast degradation and presents a long-term biocompatible biomatrix for cells, it blocks some bioactive sites of fibrinogen that can affect the biological activity of the PEGylated fibrin [37]. Therefore, PEG-NHS might bind or mask Arg-Gly-Asp sites of fibrin [31] and, as a result, change the hydrogel bioactivity [69]. It seems that with increasing the PEG:Fib molar ratio, the blocked active sites could be increased and, therefore, PEG:Fib 5:1 T50 may present more active sites. Moreover, as Shpichka et al. [24] reported, PEG:Fib 10:1 demonstrated a more compact structure than PEG:Fib 5:1, which had a loose network with various non-uniform sizes of pores. As a result, the cells encapsulated in PEG:Fib 5:1 T50 could migrate and proliferate better. On the other hand, PEG:Fib 10:1 T50 compared to PEG:Fib 5:1 T50 decreases or masks more active sites exposed to the protease enzymes, presents a compact structure, and provides a homogenous structure to maintain the uniformity of the cell population.

4. Conclusion

Preantral follicles need an environment that could support the cell–cell connections of the tightly connected follicle cells (oocyte, theca, and granulosa cells), preserve the integrity of their 3D architecture, and be suitable for the cells' growth. Based on our findings with isolated ovarian cells, it appears that PEG:Fib 10:1 T50 with preserving structural integrity, providing cell spreading uniformity, maintaining cell viability, and inducing cell proliferation can be a promising hydrogel for encapsulation of the human preantral follicles. Besides, PEG:Fib 5:1 T50 showed a significant proportion of viable cells, presenting the highest cell dynamic density among the tested groups. Therefore, two types of biodegradable and biocompatible hydrogels (PEG:Fib 10:1 T50 and PEG:Fib 5:1 T50), which demonstrated encouraging results, are potential candidates to serve as a matrix for the encapsulation of isolated human preantral follicles. An initial study in vitro, as performed here, could be the first step to analyze the survival and development of the follicles in these hydrogels.

Funding

This study was supported by grants from the Fonds National de la Recherche Scientifique de Belgique (the Excellence of Science (FNRS-EOS), number 30443682 (PhD scholarship awarded to S.M.) and Fondation Louvain (PhD scholarship awarded to A.D.).

CRediT authorship contribution statement

A. Dadashzadeh: Conceptualization, Methodology, Validation, Investigation, Data curation, Writing – original draft, Visualization. **S. Moghassemi:** Conceptualization, Formal analysis, Investigation, Writing – original draft, Visualization. **C.A. Amorim:** Resources, Writing – review & editing, Supervision, Project administration, Funding acquisition.

Declaration of competing interest

The authors declare that they have no known competing financial interests or personal relationships that could have appeared to influence the work reported in this paper.

Acknowledgments

The authors thank Dr. Lieven Desmet (from Support en Méthodologie et Calcul Statistique [SMCS-IMAQ-UCLouvain]), for his help with statistical analysis. They also thank Dolores Gonzalez, Olivier Van Kerk, and Sarah Storder for their technical assistance.

References

[1] K. Dzobo, N.E. Thomford, D.A. Senthebane, H. Shipanga, A. Rowe, C. Dandara, et al., Advances in regenerative medicine and tissue engineering: innovation and transformation of medicine, Stem Cell. Int. 2018 (2018).
[2] R. Lanza, R. Langer, J.P. Vacanti, A. Atala, Principles of Tissue Engineering, Academic Press, 2020.
[3] M.C. Chiti, M.-M. Dolmans, J. Donnez, C. Amorim, Fibrin in reproductive tissue engineering: a review on its application as a biomaterial for fertility preservation, Ann. Biomed. Eng. 45 (7) (2017) 1650–1663.
[4] P.K. Kreeger, J.W. Deck, T.K. Woodruff, L.D. Shea, The in vitro regulation of ovarian follicle development using alginate-extracellular matrix gels, Biomaterials 27 (5) (2006) 714–723.
[5] D.F. Albertini, G. Akkoyunlu, Ovarian follicle culture systems for mammals, Methods Enzymol. 476 (2010) 107–121. Elsevier.
[6] V.R. Araújo, M.O. Gastal, J.R. Figueiredo, E.L. Gastal, In vitro culture of bovine preantral follicles: a review, Reprod. Biol. Endocrinol. 12 (1) (2014) 78.
[7] A. Dadashzadeh, S. Moghassemi, A. Shavandi, C.A. Amorim, A review on biomaterials for ovarian tissue engineering, Acta Biomater. 26 (S1742-7061) (2021) 00552–00553, https://doi.org/10.1016/j.actbio.2021.08.026.
[8] D.D. Manavella, L. Cacciottola, C.M. Desmet, B.F. Jordan, J. Donnez, C.A. Amorim, et al., Adipose tissue-derived stem cells in a fibrin implant enhance neovascularization in a peritoneal grafting site: a potential way to improve ovarian tissue transplantation, Hum. Reprod. 33 (2) (2018) 270–279.
[9] M.C. Chiti, C.A. Amorim, M.-M. Dolmans, Fibrin based artificial ovary prototype: from animal models to human clinical application, Curr. Trends Clin. Embryol. 5 (3) (2018) 122–129.
[10] M.C. Chiti, M.-M. Dolmans, L. Mortiaux, F. Zhuge, E. Ouni, P.A.K. Shahri, et al., A novel fibrin-based artificial ovary prototype resembling human ovarian tissue in terms of architecture and rigidity, J. Assist. Reprod. Genet. 35 (1) (2018) 41–48.
[11] M.C. Chiti, M.M. Dolmans, O. Orellana, M. Soares, F. Paulini, J. Donnez, et al., Influence of follicle stage on artificial ovary outcome using fibrin as a matrix, Hum. Reprod. 31 (12) (2016) 2898.
[12] V. Luyckx, M.M. Dolmans, J. Vanacker, C. Legat, C. Fortuno Moya, J. Donnez, et al., A new step toward the artificial ovary: survival and proliferation of isolated murine follicles after autologous transplantation in a fibrin scaffold, Fertil. Steril. 101 (4) (2014) 1149–1156.
[13] V. Luyckx, M.-M. Dolmans, J. Vanacker, S.R. Scalercio, J. Donnez, C.A. Amorim, First step in developing a 3D biodegradable fibrin scaffold for an artificial ovary, J. Ovarian Res. 6 (1) (2013) 1–10.
[14] F. Paulini, J.M. Vilela, M.C. Chiti, J. Donnez, P. Jadoul, M.-M. Dolmans, et al., Survival and growth of human preantral follicles after cryopreservation of ovarian tissue, follicle isolation and short-term xenografting, Reprod. Biomed. Online 33 (3) (2016) 425–432.
[15] O.M. Benavides, J.P. Quinn, S. Pok, J. Petsche Connell, R. Ruano, J.G. Jacot, Capillary-like network formation by human amniotic fluid-derived stem cells within fibrin/poly (ethylene glycol) hydrogels, Tissue Eng. Part A 21 (7–8) (2015) 1185–1194.
[16] K.M. Galler, A.C. Cavender, U. Koeklue, L.J. Suggs, G. Schmalz, R.N. D'Souza, Bioengineering of dental stem cells in a PEGylated fibrin gel, Regen. Med. 6 (2) (2011) 191–200.
[17] T.A. Ahmed, E.V. Dare, M. Hincke, Fibrin: a versatile scaffold for tissue engineering applications, Tissue Eng. Part B Rev. 14 (2) (2008) 199–215.
[18] J. Kim, A.S. Perez, J. Claflin, A. David, H. Zhou, A. Shikanov, Synthetic hydrogel supports the function and regeneration of artificial ovarian tissue in mice, NPJ Regen. Med. 1 (1) (2016) 1–8.
[19] A. Shikanov, M. Xu, T.K. Woodruff, L.D. Shea, A method for ovarian follicle encapsulation and culture in a proteolytically degradable 3 dimensional system, JoVE (J. Visual. Exp.) (49) (2011) e2695.
[20] A. Shikanov, M. Xu, T.K. Woodruff, L.D. Shea, Interpenetrating fibrin–alginate matrices for in vitro ovarian follicle development, Biomaterials 30 (29) (2009) 5476–5485.
[21] M. Xu, A.T. Fazleabas, A. Shikanov, E. Jackson, S.L. Barrett, J. Hirshfeld-Cytron, et al., In vitro oocyte maturation and preantral follicle culture from the luteal-phase baboon ovary produce mature oocytes, Biol. Reprod. 84 (4) (2011) 689–697.
[22] G. Zhang, X. Wang, Z. Wang, J. Zhang, L. Suggs, A PEGylated fibrin patch for mesenchymal stem cell delivery, Tissue Eng. 12 (1) (2006) 9–19.
[23] D. Dikovsky, H. Bianco-Peled, D. Seliktar, Proteolytically degradable photopolymerized hydrogels made from PEG–fibrinogen adducts, Adv. Eng. Mater. 12 (6) (2010) B200–B209.
[24] A. Shpichka, A. Koroleva, A. Deiwick, P. Timashev, E. Semenova, I.Y. Moiseeva, et al., Evaluation of the vasculogenic potential of hydrogels based on modified fibrin, Cell Tissue Biol. 11 (1) (2017) 81–87.
[25] P.B. Lawrence, J.L. Price, How PEGylation influences protein conformational stability, Curr. Opin. Chem. Biol. 34 (2016) 88–94.
[26] A. Jain, S.K. Jain, PEGylation: an approach for drug delivery. A review, Crit. Rev. Ther. Drug Carrier Syst. 25 (5) (2008).
[27] C.T. Drinnan, G. Zhang, M.A. Alexander, A.S. Pulido, L.J. Suggs, Multimodal release of transforming growth factor-β1 and the BB isoform of platelet derived growth factor from PEGylated fibrin gels, J. Contr. Release 147 (2) (2010) 180–186.
[28] T.H. Barker, G.M. Fuller, M.M. Klinger, D. Feldman, J. Hagood, Modification of fibrinogen with poly (ethylene glycol) and its effects on fibrin clot characteristics, J. Biomed. Mater. Res.: Offic. J. Soc. Biomater. Japan. Soc. Biomater. Austr. Soc. Biomater. Kor. Soc. Biomater. 56 (4) (2001) 529–535.
[29] G. Zhang, C.T. Drinnan, L.R. Geuss, L.J. Suggs, Vascular differentiation of bone marrow stem cells is directed by a tunable three-dimensional matrix, Acta Biomater. 6 (9) (2010) 3395–3403.
[30] S. Seetharaman, S. Natesan, R.S. Stowers, C. Mullens, D.G. Baer, L.J. Suggs, et al., A PEGylated fibrin-based wound dressing with antimicrobial and angiogenic activity, Acta Biomater. 7 (7) (2011) 2787–2796.
[31] A. Shpichka, P. Konarev, Y.M. Efremov, A. Kryukova, N. Aksenova, S. Kotova, et al., Digging deeper: structural background of PEGylated fibrin gels in cell migration and lumenogenesis, RSC Adv. 10 (8) (2020) 4190–4200.
[32] J. Gil, S. Natesan, J. Li, J. Valdes, A. Harding, M. Solis, et al., A PEGylated fibrin hydrogel-based antimicrobial wound dressing controls infection without impeding wound healing, Int. Wound J. 14 (6) (2017) 1248–1257.
[33] D.O. Zamora, S. Natesan, S. Becerra, N. Wrice, E. Chung, L.J. Suggs, et al., Enhanced wound vascularization using a dsASCs seeded FPEG scaffold, Angiogenesis 16 (4) (2013) 745–757.
[34] A. Koroleva, A. Deiwick, A. Nguyen, R. Narayan, A. Shpichka, O. Kufelt, et al., Hydrogel-based microfluidics for vascular tissue engineering, BioNanoMaterials 17 (1–2) (2016) 19–32.
[35] Z. Li, J. Guan, Hydrogels for cardiac tissue engineering, Polymers 3 (2) (2011) 740–761.
[36] M. Gonen-Wadmany, L. Oss-Ronen, D. Seliktar, Protein–polymer conjugates for forming photopolymerizable biomimetic hydrogels for tissue engineering, Biomaterials 28 (26) (2007) 3876–3886.
[37] D. Dikovsky, H. Bianco-Peled, D. Seliktar, The effect of structural alterations of PEG-fibrinogen hydrogel scaffolds on 3-D cellular morphology and cellular migration, Biomaterials 27 (8) (2006) 1496–1506.
[38] K. Shapira-Schweitzer, D. Seliktar, Matrix stiffness affects spontaneous contraction of cardiomyocytes cultured within a PEGylated fibrinogen biomaterial, Acta Biomater. 3 (1) (2007) 33–41.
[39] D.K. Jarrell, E.J. Vanderslice, M.L. Lennon, A.C. Lyons, M.C. VeDepo, J.G. Jacot, Increasing salinity of fibrinogen solvent generates stable fibrin hydrogels for cell delivery or tissue engineering, PLoS One 16 (5) (2021), e0239242.
[40] E. Chung, S.Y. Nam, L.M. Ricles, S.Y. Emelianov, L.J. Suggs, Evaluation of gold nanotracers to track adipose-derived stem cells in a PEGylated fibrin gel for dermal tissue engineering applications, Int. J. Nanomed. 8 (2013) 325.
[41] L.R. Geuss, A.C. Allen, D. Ramamoorthy, L.J. Suggs, Maintenance of HL-1 cardiomyocyte functional activity in PEGylated fibrin gels, Biotechnol. Bioeng. 112 (7) (2015) 1446–1456.
[42] H. Liu, S.F. Collins, L.J. Suggs, Three-dimensional culture for expansion and differentiation of mouse embryonic stem cells, Biomaterials 27 (36) (2006) 6004–6014.
[43] R. Jin, L.M. Teixeira, P.J. Dijkstra, M. Karperien, C. Van Blitterswijk, Z. Zhong, et al., Injectable chitosan-based hydrogels for cartilage tissue engineering, Biomaterials 30 (13) (2009) 2544–2551.
[44] M. Gallardo, F. Paulini, A. Corral, M. Balcerzyk, C.M. Lucci, J. Ambroise, et al., Evaluation of a new freezing protocol containing 20% dimethyl sulphoxide concentration to cryopreserve human ovarian tissue, Reprod. Biomed. Online 37 (6) (2018) 653–665.
[45] P. Asiabi, M.-M. Dolmans, J. Ambroise, A. Camboni, C. Amorim, In vitro differentiation of theca cells from ovarian cells isolated from postmenopausal women, Hum. Reprod. 35 (12) (2020) 2793–2807.
[46] V. Feisst, A.E. Brooks, C.-J.J. Chen, P.R. Dunbar, Characterization of mesenchymal progenitor cell populations directly derived from human dermis, Stem Cell. Dev. 23 (6) (2014) 631–642.
[47] D. da-Silva-Freitas, J. Boldrini-França, E. Candiani Arantes, PEGylation: a successful approach to improve the biopharmaceutical potential of snake venom thrombin-like serine protease, Protein Pept. Lett. 22 (12) (2015) 1133–1139.
[48] B. Plesner, C.J. Fee, P. Westh, A.D. Nielsen, Effects of PEG size on structure, function and stability of PEGylated BSA, Eur. J. Pharm. Biopharm. 79 (2) (2011) 399–405.
[49] F.M. Veronese, G. Pasut, PEGylation, successful approach to drug delivery, Drug Discov. Today 10 (21) (2005) 1451–1458.
[50] P.L. Turecek, M.J. Bossard, F. Schoetens, I.A. Ivens, PEGylation of biopharmaceuticals: a review of chemistry and nonclinical safety information of approved drugs, J. Pharmaceut. Sci. 105 (2) (2016) 460–475.
[51] R. Mooney, B. Tawil, M. Mahoney, Specific fibrinogen and thrombin concentrations promote neuronal rather than glial growth when primary neural cells are seeded within plasma-derived fibrin gels, Tissue Eng. Part A 16 (5) (2010) 1607–1619.

[52] M. Carr Jr., B. Alving, Effect of fibrin structure on plasmin-mediated dissolution of plasma clots, Blood Coagul. Fibrinolysis: Int. J. Haemost. Thromb. 6 (6) (1995) 567–573.
[53] B. Blombäck, K. Carlsson, K. Fatah, B. Hessel, R. Procyk, Fibrin in human plasma: gel architectures governed by rate and nature of fibrinogen activation, Thromb. Res. 75 (5) (1994) 521–538.
[54] S.L. Rowe, S. Lee, J.P. Stegemann, Influence of thrombin concentration on the mechanical and morphological properties of cell-seeded fibrin hydrogels, Acta Biomater. 3 (1) (2007) 59–67.
[55] J. Collet, D. Park, C. Lesty, J. Soria, C. Soria, G. Montalescot, et al., Influence of fibrin network conformation and fibrin fiber diameter on fibrinolysis speed: dynamic and structural approaches by confocal microscopy, Arterioscler. Thromb. Vasc. Biol. 20 (5) (2000) 1354–1361.
[56] M.S. Mazzeo, T. Chai, M. Daviran, K.M. Schultz, Characterization of the kinetics and mechanism of degradation of human mesenchymal stem cell-laden poly(ethylene glycol) hydrogels, ACS Appl. Bio Mater. 2 (1) (2019) 81–92.
[57] M.Y. Shie, J.J. Lee, C.C. Ho, S.Y. Yen, H.Y. Ng, Y.W. Chen, Effects of gelatin methacrylate bio-ink concentration on mechano-physical properties and human dermal fibroblast behavior, Polymers (Basel) 12 (9) (2020).
[58] M. Zhu, Y. Wang, G. Ferracci, J. Zheng, N.J. Cho, B.H. Lee, Gelatin methacryloyl and its hydrogels with an exceptional degree of controllability and batch-to-batch consistency, Sci. Rep. 9 (1) (2019) 6863.
[59] L. Papa, M. Djedaini, T.C. Martin, M. Zangui, K.G. Beaumont, R. Sebra, et al., Limited mitochondrial activity coupled with strong expression of CD34, CD90 and EPCR determines the functional fitness of ex vivo expanded human hematopoietic stem cells, Front. Cell Develop. Biol. 8 (2020).
[60] M. Dominici, K. Le Blanc, I. Mueller, I. Slaper-Cortenbach, F. Marini, D. Krause, et al., Minimal criteria for defining multipotent mesenchymal stromal cells. The International Society for Cellular Therapy position statement, Cytotherapy 8 (4) (2006) 315–317.
[61] G. Zhang, Q. Hu, E.A. Braunlin, L.J. Suggs, J. Zhang, Enhancing efficacy of stem cell transplantation to the heart with a PEGylated fibrin biomatrix, Tissue Eng. Part A 14 (6) (2008) 1025–1036.
[62] Y. Kirilak, N.J. Pavlos, C.R. Willers, R. Han, H. Feng, J. Xu, et al., Fibrin sealant promotes migration and proliferation of human articular chondrocytes: possible involvement of thrombin and protease-activated receptors, Int. J. Mol. Med. 17 (4) (2006) 551–558.
[63] K. Tani, S. Yasuoka, F. Ogushi, K. Asada, K. Fujisawa, T. Ozaki, et al., Thrombin enhances lung fibroblast proliferation in bleomycin-induced pulmonary fibrosis, Am. J. Respir. Cell Mol. Biol. 5 (1) (1991) 34–40.
[64] V. Borrelli, A.V. Sterpetti, P. Coluccia, B. Randone, A. Cavallaro, L.S. D'Angelo, et al., Bimodal concentration-dependent effect of thrombin on endothelial cell proliferation and growth factor release in culture, J. Surg. Res. 100 (2) (2001) 154–160.
[65] C. McNamara, I. Sarembock, L. Gimple, Jn Fenton, S. Coughlin, G. Owens, Thrombin stimulates proliferation of cultured rat aortic smooth muscle cells by a proteolytically activated receptor, J. Clin. Invest. 91 (1) (1993) 94–98.
[66] L. Oss-Ronen, D. Seliktar, Polymer-conjugated albumin and fibrinogen composite hydrogels as cell scaffolds designed for affinity-based drug delivery, Acta Biomater. 7 (1) (2011) 163–170.
[67] K. Webb, V. Hlady, P.A. Tresco, Relative importance of surface wettability and charged functional groups on NIH 3T3 fibroblast attachment, spreading, and cytoskeletal organization, J. Biomed. Mater. Res.: Offic. J. Soc. Biomat. Japan. Soc. Biomater. Austr. Soc. Biomater. 41 (3) (1998) 422–430.
[68] B.H. Lee, S.P.H. Tin, S.Y. Chaw, Y. Cao, Y. Xia, T.W. Steele, et al., Influence of soluble PEG-OH incorporation in a 3D cell-laden PEG-fibrinogen (PF) hydrogel on smooth muscle cell morphology and growth, J. Biomater. Sci. Polym. Ed. 25 (4) (2014) 394–409.
[69] M. Gonen-Wadmany, R. Goldshmid, D. Seliktar, Biological and mechanical implications of PEGylating proteins into hydrogel biomaterials, Biomaterials 32 (26) (2011) 6025–6033.